Integrated Regional Resilience Assessment Platform for Interdependent Systems

Jinyan Zhao[a,*], Nikola Blagojević[b], Sina Naeimi[a], Barbaros Cetiner[a], Tianyu Han[a], Frank McKenna[a], Božidar Stojadinović[c] and Matthew DeJong[a]

[a]NHERI-SimCenter, University of California, Berkeley, CA, USA
[b]Dept. of Civil and Environmental Engineering, Stanford University, USA
[c]Dept. of Civil, Environmental, and Geomatic Engineering, ETH Zürich, Switerland

ARTICLE INFO

Keywords:
Infrastructure resilience
Computer simulations
Regional-scale
Open source
Application programming interfaces

ABSTRACT

Computer simulations are critical for assessing the resilience of civil infrastructure to natural hazards. To support efficient and comprehensive analyses that account for interdependencies among infrastructure systems, an integrated platform that spans the full resilience evaluation process, from damage to recovery, is essential. This paper presents such a platform by linking SimCenter's R2D tool, together with embedded infrastructure system operation simulators, to the recovery simulator pyrecodes. Compared to state-of-the-art post-disaster recovery simulation tools, the proposed platform offers three key advantages: first, it employs high-fidelity traffic flow and potable water delivery simulators to improve the accuracy of resource allocation and the representation of system interdependencies in recovery simulations; second, it streamlines continuous system performance evaluation for interdependent systems considering the change in both resource supply and demand, thereby facilitating quantitative assessment of system resilience; and third, it provides an integrated open-source framework that supports reconfiguration and extension, enabling the continuous incorporation of newer and more advanced regional-scale simulators and allowing flexible levels of simulation fidelity across infrastructure systems. Thus, the proposed simulation platform establishes a unique and foundational framework for future integrated regional resilience modeling and assessment. The integration is achieved through two application programming interfaces (APIs): one connecting regional damage and recovery simulators, and the other linking the recovery simulator with infrastructure-specific service generation and dispatch (operation) simulators. The resulting open-source platform provides a user-friendly interface for hazard, exposure, vulnerability, and recovery analysis, as well as resilience quantification. The platform's utility is demonstrated in a case study of a California community subjected to an M_w 7.0 earthquake, where damage and recovery of buildings, bridges, tunnels, roadways, and water distribution pipelines are simulated. The case study illustrates the ability of the tools to quantify resilience comprehensively with high spatial and temporal resolution. Although only one case study and two system operation simulators are presented, the APIs are designed to integrate a broad range of hazard, exposure, damage, recovery, and operation simulators (e.g., PyPSA and pandapower for power system modeling), beyond those featured here.

1. Introduction

Assessing the resilience of civil infrastructure to natural hazards at a community or regional scale is critical for developing emergency response plans, prioritizing retrofit and mitigation measures, and setting insurance premiums. Computer simulations play a central role in enabling such resilience assessments.

Community- and regional-scale resilience assessment research generally falls into four categories: hazard analysis, exposure analysis, vulnerability analysis, and recovery analysis. Several research-oriented simulation tools are available for each of these categories. For example, OpenSHA [22], OpenQuake [36], EQSIM [28], and ADCIRC [26] are widely used for hazard simulations related to earthquakes and storm surges. While OpenQuake and EQSIM also support vulnerability analysis, they primarily model infrastructure components (e.g., buildings and bridges) individually, with limited capability for system-level performance assessments and no recovery modeling. To evaluate post-disaster system-level performance (e.g., transportation service provision), proprietary infrastructure models are often

*Corresponding author
jinyan_zhao@berkeley.edu (J. Zhao)
ORCID(s):

employed based on the results of individual component analyses. Recent advances in tools such as IN-CORE [24] and SimCenter's R2D [29] have integrated hazard analysis, exposure modeling tools (e.g. BRAILS++ [14]), and system-level infrastructure vulnerability analysis, allowing simulation of damage and loss of interdependent infrastructure systems immediately after a hazard event. Additionally, pyrecodes [12] has been developed by researchers at ETH Zurich as an open-source software tool for post-disaster recovery simulations.

Despite the increasing need for community resilience assessment (e.g., [37]), an integrated open-source, modular platform that spans all four analysis categories at the regional scale, and particularly one that allows the readily integration of newly developed and higher fidelity simulators for the hazard, the structures, and the infrastructure systems, is still lacking. Furthermore, recovery simulators are rarely coupled with infrastructure operation simulators, making it difficult to assess the dynamics of infrastructure performance during post-disaster recovery using physically rigorous simulators. The absence of such an integrated simulation platform limits the realism and comprehensiveness of current community disaster resilience analyses. For example, building and household recovery subject to repair priority and recovery resource constraints (e.g., financing and reconstruction crews) were simulated in [47, 45, 16, 3]. However, the post-disaster damage and reduced serviceability of infrastructure systems were not taken into account. Similarly, the restoration of a water system following an earthquake was simulated in [40], but the interdependency between the water system and housing and other infrastructure was not considered, and the post-disaster water demand was assumed to remain constant relative to the pre-earthquake level. Roadway accessibilities of hospitals and buildings considering bridge damages were evaluated in [13, 15], while functional recovery of buildings with disruptions to cross-dependent utility networks was simulated in [27]. However, these studies relied on simplified transportation and utility network functionality evaluations using topological analysis or discrete-event analysis, while infrastructure performance analysis based on traffic flow theories or hydraulic laws remained absent.

This paper aims to address these gaps by integrating different hazard, exposure, vulnerability and recovery simulators, which may have originally been designed to function as stand-alone applications, into a unified framework for regional resilience assessment. The key enabling component is a set of application programming interfaces (APIs) that connect SimCenter's R2D damage simulator, pyrecodes recovery simulator, REWET potable water distribution simulator, and the Residual Demand traffic flow simulator into a unified platform. The APIs are carefully designed to balance computational efficiency, stability, and flexibility, so that a wide range of infrastructure system operation simulators can be employed to simulate recovery resource allocations, thereby facilitating decision-making with unprecedented resolution. Although only two infrastructure simulators are discussed in this paper, the proposed APIs establish a flexible framework that can be transported to simulation tools beyond those presented herein. Compared to existing recovery simulators, the proposed simulation platform is tightly coupled with infrastructure system operation simulators, enabling more realistic system performance assessments than the topological- or dependency ruleset–based analyses commonly used in recovery simulations in the literature. Integrating system operation simulators also enhances the accuracy of resource allocation and distribution analysis, which enables the evaluation of quantitative resilience metrics characterized by the amount of unmet demand throughout the recovery process. Compared to existing damage and system operation simulators, this tight coupling with the recovery simulator enables continuous evaluation of system performance while accounting for variations in system demand and cross-system interdependencies during the recovery process, thereby providing more quantitative and intuitive system-level resilience metrics.

The remainder of this paper is structured as follows. Section 2 introduces the integrated simulation workflow, which includes a background introduction to the damage simulator R2D and recovery simulator pyrecodes, as well as the APIs that enable their integration. Section 3 presents a case study that demonstrates the application of the proposed simulation platform. Finally, the advantages of the proposed simulation framework are discussed.

2. Resilience Assessment Platform Integration

The framework of the developed simulation platform is modularized into five main modules: a hazard analysis module, an exposure analysis module, a vulnerability analysis module, a recovery analysis module, and a resilience quantification module (see Fig. 1). Specifically, the hazard analysis module quantifies the intensities of natural hazards that may affect a region, while the exposure evaluation module develops inventories of infrastructure that may be impacted by these hazards. The vulnerability analysis module includes structural response, damage, and loss analysis, which assesses the physical condition of the infrastructure immediately following natural hazard events. The hazard, exposure, and vulnerability modules together form the traditional risk assessment workflow, producing damage and loss metrics. For the purpose of the integrated computational platform presented in this paper, these three modules are

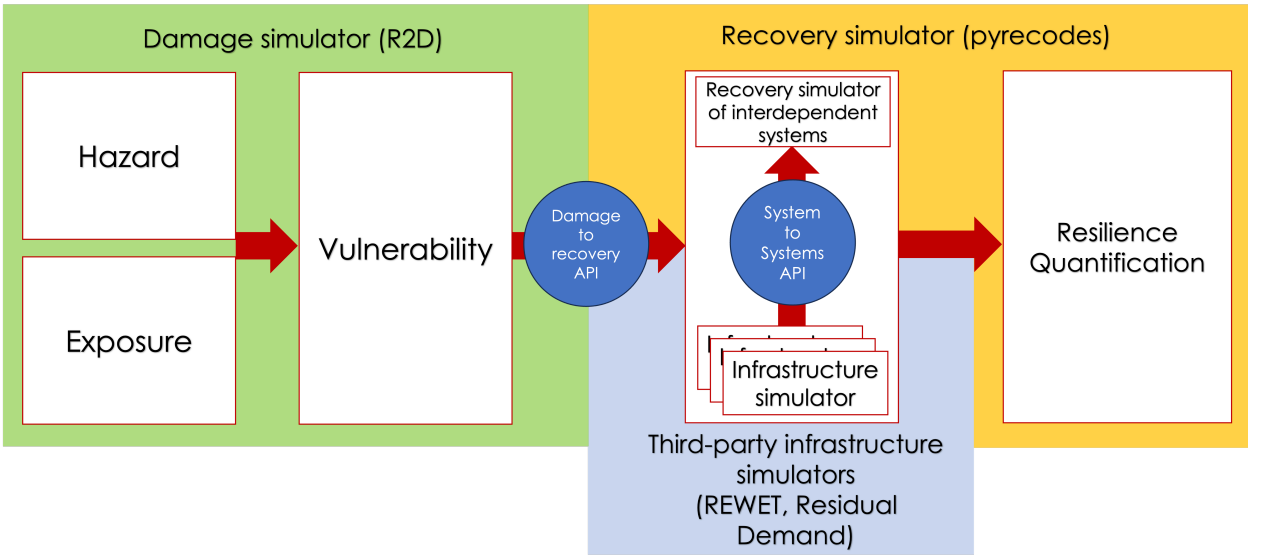

Figure 1: Computational framework of the proposed integrated resilience assessment platform facilitated by the damage-to-recovery API and system-to-systems API

collectively labeled the 'Damage simulator' (the green block in Fig. 1), as its primary output relevant for the regional resilience assessment is physical damage to infrastructure components.

The recovery analysis module simulates the recovery of interdependent systems from damage, while the resilience quantification module provides metrics that characterize the recovery process and system resilience. The performance of individual infrastructure systems within the regional "system of interdependent systems" recovery simulator can be assessed using an infrastructure-specific service generation and dispatch (operation) simulator. For the purposes of the integrated regional resilience assessment platform presented here, the recovery module, resilience quantification module, and the associated infrastructure operation simulators are collectively labeled as the 'Recovery simulator' (the yellow block in Fig. 1).

One of the main contributions of this paper is the development of two Application Programming Interfaces (APIs) that facilitate (1) the integration between the damage and recovery simulators and (2) the integration of infrastructure-specific simulators into the regional recovery systems-of-interdependent-systems simulator. These APIs enable the creation of realistic simulations of infrastructure system operation and resource distribution during recovery, leading to more reliable assessments of recovery and resilience.

The integrated computational platform presented here combines the risk assessment framework from the R2D software [29], developed by the NHERI-SimCenter, representing the damage simulator, with pyrecodes [12], representing the regional recovery simulator. Additionally, the recovery simulator is enhanced through the integration of two infrastructure operation simulators: REWET for the potable water supply system and Residual Demand for the transportation network. The remainder of this section is organized as follows. Section 2.1 and 2.2 introduce the existing functionality of the damage simulator, R2D, and the recovery simulator, pyrecodes, which are the bases for this work. Section 2.3 presents the interface developed in this paper, which links the damage and recovery simulators. Section 2.4 reviews how component- and system-level interdependencies are modeled in pyrecodes and highlights current limitations. Finally, section 2.5 introduces the general API that integrates infrastructure simulators into the regional recovery system-of-systems model, and sections 2.6 and 2.7 present two examples of interfacing the traffic flow simulator, Residual Demand, and the water simulator, REWET, with the presented platform.

2.1. R2D damage simulator

This paper adopts the hazard, exposure, and vulnerability analysis methods from the existing version of the R2D software [29], shown in the green 'Damage simulator' block in Fig. 1. To facilitate hazard analysis, two tools have been developed in R2D: an earthquake ground motion tool and a hurricane wind speed tool. The earthquake ground motion tool integrates earthquake rupture forecasting models, empirical ground motion models, and spatial correlation

models to generate earthquake ground motion intensity measure (IM) samples at user-defined locations. The hurricane wind speed tool enables users to define a hurricane track and landfall parameters, and use an analytical wind speed model [38] to generate wind speed realizations. Additionally, R2D supports importing intensity measures from other hazard analysis tools, such as USGS ShakeMap [44] and ADCIRC [26], using common GIS formats. For a full list of hazard analysis tools in R2D, see [31].

Exposure analysis in R2D involves defining an inventory of infrastructure systems that may be affected by the studied hazard and estimating the hazard intensity at each infrastructure component through geospatial analysis. Region-specific asset information must be collected with sufficient granularity and scope to meet the requirements for vulnerability and recovery analysis. A variety of open data sources, such as those summarized in [4], can be utilized to create the inventory. To streamline this process, an inventory creation tool, BRAILS++ [14], can be run using R2D's graphical interface.

Vulnerability analysis in R2D comprises both structural response analysis and damage analysis. Any structural analysis tool accessible through Python can be used for structural response analysis within R2D. Subsequently, a damage and loss (DL) analysis is performed, determining the damage of the infrastructure components based on the estimated structural responses. This DL analysis is achieved using the open-source Python package Pelicun3 [51], which uses either a built-in DL model database or user-defined DL databases. Using the built-in DL models, R2D can perform vulnerability analysis at a high spatial resolution using FEMA's HAZUS methodology under the impact of earthquakes, hurricanes, and floods. Alternatively, R2D also includes higher-fidelity analysis models, e.g., [25] and [48], that evaluate story-level damage states for buildings under earthquake effects. Other modeling methodologies can be implemented with additional user input and relatively simple programming, thanks to R2D's open-source, modular design. A full list of features available in R2D can be found at [30].

2.2. pyrecodes recovery simulator

The pyrecodes regional recovery simulator, shown in the yellow 'Recovery simulator' block of Fig. 1, models the recovery of individual infrastructure components while capturing system-level interdependencies through the simulation of resource flows among components. Pyrecodes requires component damage states as input, which are provided by the API linking to the 'Damage simulator' (see section 2.3). At the component level, recovery is represented as a sequence of activities (e.g., demolition, construction) and impeding factors (e.g., inspection, design, permitting) that influence recovery times [11]. This sequence is conditioned on the component's characteristics (e.g., occupancy type, construction type) and its initial post-disaster damage. Each impeding factor and recovery activity is characterized by the preceding activities that must be completed before the activity can begin, along with the activities' duration and resource demands. A suite of resource supply and demand parameters is also defined for each component. A component's demand is categorized into operational demand and recovery demand. Operational demand (e.g., water and electricity) must be satisfied for the component to remain functional, while recovery demand (e.g., materials, funding) must be met before recovery activities can begin. The supply represents the resources a component contributes to the community (e.g., a building provides shelter). A component's ability to supply resources depends on whether its operational demand is met and whether it has reached a predefined recovery stage.

At the system level, pyrecodes simulates the interdependencies among components at each time step of the recovery process by modeling component interaction as the flow of resources among components. The interdependency modeling is detailed in section 2.4.

Several resilience calculators are available in pyrecodes, providing different system recovery and resilience metrics. These metrics are obtained by aggregating simulated component-level recovery trajectories allowing for scenario-based system recovery time assessment, unmet resource demand, or NIST's resilience goals [7, 9]. The resilience calculators can also be extended to include risk-based metrics [8].

2.3. Damage-to-recovery API

The damage simulator estimates the condition of all components immediately after a hazard event. The resulting damage and exposure information, which includes component characteristics relevant to recovery, is transferred to the recovery simulator through the damage-to-recovery API, as illustrated in Fig. 2. This API operates in two steps: first, it converts and saves the damage and exposure data into a JSON file, and second, it parses this file into a format that the recovery simulator (i.e., pyrecodes) can process, enabling it to assign damage states and component characteristics to interdependent infrastructure systems.This interface enables an end-to-end framework spanning from hazard analysis

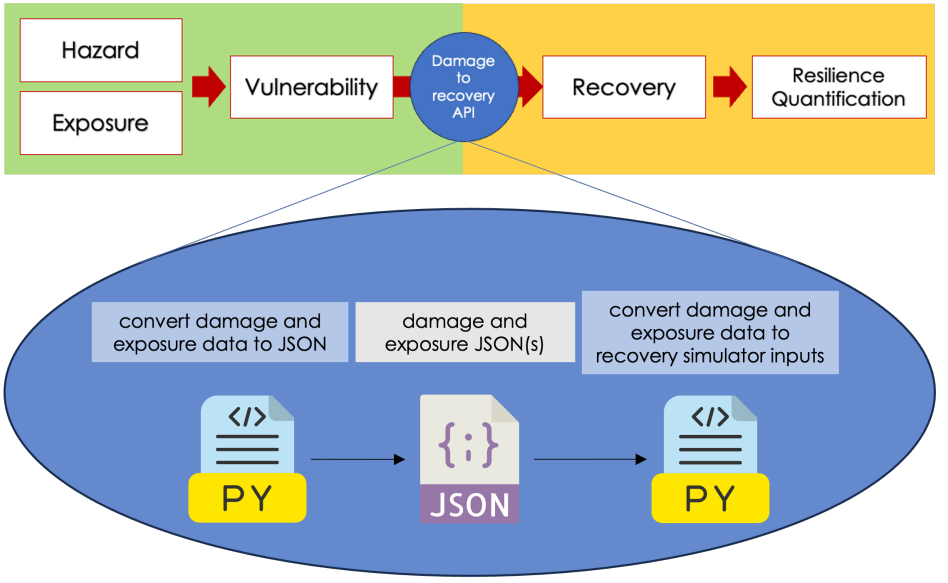

Figure 2: Damage-to-recovery API

to recovery analysis, providing a user-friendly simulation workflow that can support resilience-metrics–based risk assessment, sensitivity analysis, and network optimization.

2.4. Interdependency modeling in pyrecodes

Fig. 3 shows the pyrecodes recovery simulation algorithm in detail on the left. Once the damage is assigned to components, the recovery simulation starts as a time-stepping loop where, at each step, three actions are taken. First, the supply and demand of all components are updated considering their damage state at the time step. Then, resources are distributed among components using resource distribution models to determine whether the components' recovery and operation demands can be met by the supply available at the time step. Components with sufficient recovery resources can proceed with their recovery activities, while components that do not receive enough resources will wait for the next time step. The simulation continues until all components have completed their recovery activities or a time step limit is reached.

The resource distribution models in pyrecodes are simple and based on the connectivity between localities, components' supply capacities and demand and a user-defined priority relationship [9]. This resource distribution approach has been shown to effectively model recovery resource constraints, dynamic component interdependencies and cascading effects , and the impact of infrastructure systems on buildings' functional recovery [11, 9, 10]. However, resource distribution models in the existing pyrecodes ignore or simplify physical and technical laws related to the operation of infrastructure systems (e.g., water head equilibrium and quantity conservation, electricity voltage and current limits, etc.). Furthermore, system-level performance metrics, such as average travel time delay and water delivery quantities to households, are often desired for evaluating the resilience of infrastructure systems but cannot be provided by the current implementation of pyrecodes.

To address these limitations, the system-to-systems API shown in Fig. 3 was created. This API facilitates the integration of better infrastructure-specific simulators into the recovery simulation. These infrastructure simulators model the operation of infrastructure systems and provide the information on the ability of a given infrastructure system to provide resources to components of various other infrastructure systems at different time steps of the recovery simulation.

Recent developments in R2D have enabled the operation simulation and performance evaluation for damaged water distribution networks [34] and damaged transportation networks [49] immediately after natural hazard events and during recovery. To enable dynamic infrastructure assessment and more reliable system interdependency modeling, these system operation simulators are incorporated into the recovery simulation framework, as detailed in section 2.5.

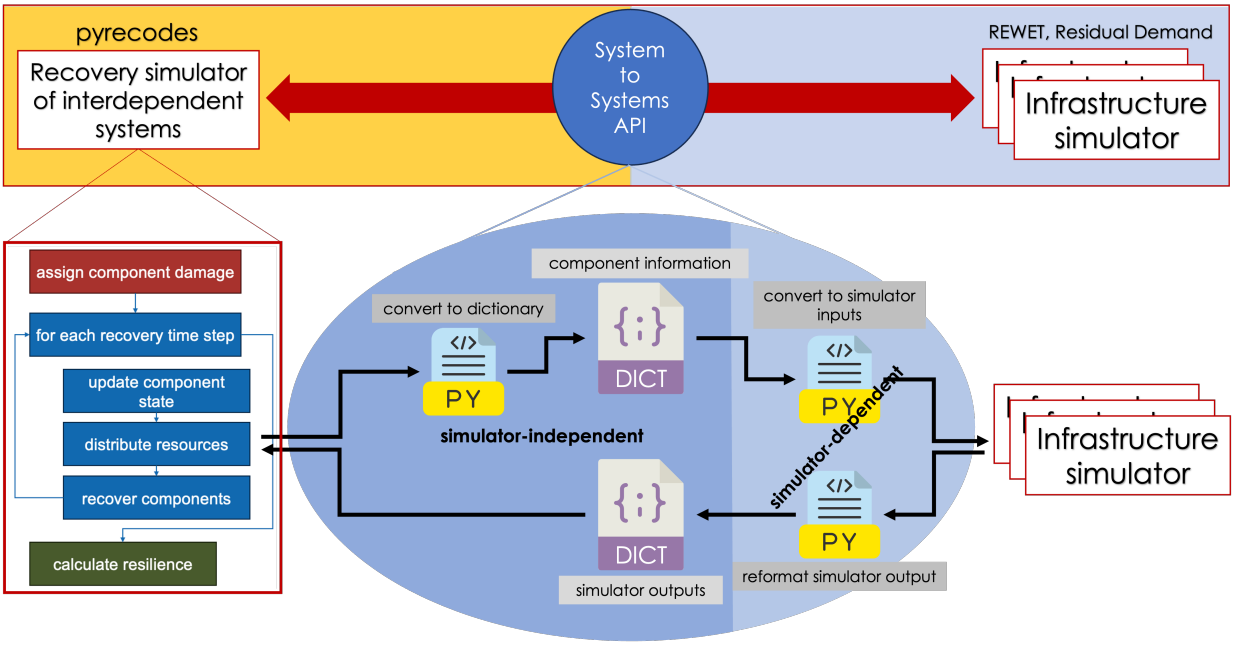

Figure 3: pyrecodes algorithm and the system-to-systems API that interfaces infrastructure simulators into the system-of-interdependent-systems

2.5. System-to-systems API

Infrastructure simulators are invoked during the "distribute resources" stage of pyrecodes' recovery simulation (see the left part of Fig. 3). After updating the component damage states based on the results of the previous recovery time-step, the "convert to dictionary" API function (Darker blue part at the center of Fig. 3) is called to collect information from all infrastructure components in pyrecodes and store the required data (e.g., recovery stage, functional level, and other relevant characteristics) into a Python dictionary (i.e., DICT) mirroring the structure of the exposure JSON file used as the input for the recovery simulator (section 2.3). This section of the API is universal to all infrastructure simulators, and is depicted as "simulator-independent" part of the API (dark blue color in the center of Fig. 3). The dictionary is then read by the "convert to simulator inputs" API function (the lighter blue part at the center of Fig. 3), which provides the component status information to the infrastructure simulator, synchronizing it with the current component recovery progress. Synchronization typically involves updating the topology of the infrastructure systems and adjusting the capacities of various components based on their current state of damage and recovery. The infrastructure simulator subsequently evaluates system performance and sends system-level performance metrics back to pyrecodes (e.g., a dictionary containing the percent of met water demand for each component or travel times between components) as a dictionary using the "reformat simulator output" API function, enabling dynamic infrastructure system operation assessments throughout the recovery process. Such infrastructure operation simulators replace simple resource distribution models currently implemented in pyrecodes. Note that, to accommodate the different input and output formats of the infrastructure simulators, the section of the API that converts the component information contained in the dictionary into inputs for the infrastructure simulator and transforms simulator outputs into pyrecodes-readable data differs for each infrastructure simulator, and is thus labeled as "simulator-dependent".

Given that infrastructure operation simulators can be computationally expensive, pyrecodes allows the evaluation of each infrastructure simulator at a set of different selected time steps. The system operation condition from the previous evaluation is used to approximate the system operation condition during the intervening time steps. This approach enables efficient resilience evaluation with a small loss of accuracy.

At the time of writing, two infrastructure simulators have been interfaced with pyrecodes: the traffic flow simulator, Residual Demand [49], which provides system-level traffic performance metrics, and the potable water distribution simulator, REWET [34], which supports both system performance evaluation and advanced resource distribution

simulations. The following two sections present the interfacing of the two infrastructure simulators in detail, and additional infrastructure simulators can be incorporated following these two examples.

2.6. Interfacing Residual Demand traffic flow simulator with pyrecodes

The Residual Demand traffic flow simulator is employed in this paper to simulate the operation of the roadway network and evaluate its performance from initial damage to the completion of the recovery process. At predefined time steps, the simulator-independent system-to-systems API transmits the status of all buildings and transportation network components to the Residual Demand simulator. The "convert to simulator inputs" API function then provides the current state of buildings and transportation components to the traffic flow simulator. This information is used to infer both the transportation service demand and transportation service supply, as well as to simulate the traffic flow. The API design allows users to modify the rule sets that infer post-disaster transportation demand and supply based on the state of buildings and transportation components. Examples of these rule sets are presented in section 3.2. This API allows a modeler to estimate the variation of traffic demand during the recovery process using dynamically simulated housing functionalities, which provides a novel approach to the active research topic of post-disaster traffic demand estimation [2].

Once the updated transportation demand and supply are estimated, the Residual Demand simulator uses a pseudo-dynamic traffic assignment algorithm to estimate the travel time for each trip. After completing the traffic assignment simulation, the travel times are provided to pyrecodes for evaluating traffic network performance. If the post-disaster travel time exceeds a predefined threshold, the traveler is likely to cancel the trip or select an alternative mode of transportation, resulting in an incomplete trip. The discrepancy between the total number of trips in the traffic demand and the number of completed trips is used to measure the resilience of the traffic network.

Additional transportation system performance metrics (e.g., those reviewed by [50]) can also be incorporated in pyrecodes. This integration of Residual Demand with the R2D-pyrecodes framework enables the dynamic evaluation of post-disaster traffic demand and network capacity. It also offers opportunities to capture infrastructure interdependencies in post-disaster travel behavior modeling, which enables more realistic transportation infrastructure resilience assessments. Example results of the dynamic resilience assessment are presented in section 3.2.

2.7. Interfacing REWET potable water distribution simulator with pyrecodes

REWET is used to evaluate the performance of the Water Distribution Network (WDN) from initial damage through to the end of recovery. Similar to the traffic flow simulator, at each simulation time step, the simulator-independent API sends the state of the WDN components and buildings to REWET. Buildings are associated to demand nodes within REWET to define the spatial granularity on which water demand is estimated. Water demand per node is estimated in proportion to the population and functionality of the buildings associated with that node.

Using the information provided by the API, alongside other predefined parameters (e.g., simulation time and hydraulic solver parameters), REWET reconfigures the network, simulates the water flow, and estimates the water supply for each demand node. To reconfigure the network, REWET modifies the network by modeling leak points and cutting off break points based on the pipeline status and a user-defined leak model. The cut-off is modeled by applying the maximum applicable leak on both sides of the break point on the pipe. REWET simulates water distribution using either EPANET V2.2 [43] or WNTR Solver [23] based on the user's selection. The amount of water delivered to each demand node is calculated, and the ratio of the amount of water supply to demand is estimated for each demand node. It is assumed that all buildings within the same demand node experience the same water supply/demand ratio. This water supply/demand ratio is sent to pyrecodes through the REWET simulator dependent API. Pyrecodes uses the ratio to describe if a building's water demand is satisfied and if a building can be restored to a functional condition.

3. Case Study

The following section illustrates the application of the presented simulation platform by assessing the resilience of Alameda Island (one of SimCenter's regional simulation testbed [6]) following a hypothetical earthquake event.

3.1. Hazard scenario, exposure, and vulnerability analysis

The studied hazard scenario is an M_w 7.0 earthquake on the Hayward Fault (Fig. 4), which is one of the earthquake rupture scenarios predicted by the USGS UCERF2 earthquake rupture forecasting model [21]. The ground shaking intensity measures (IMs), including peak ground acceleration (PGA), peak ground velocity (PGV), and pseudo-spectral

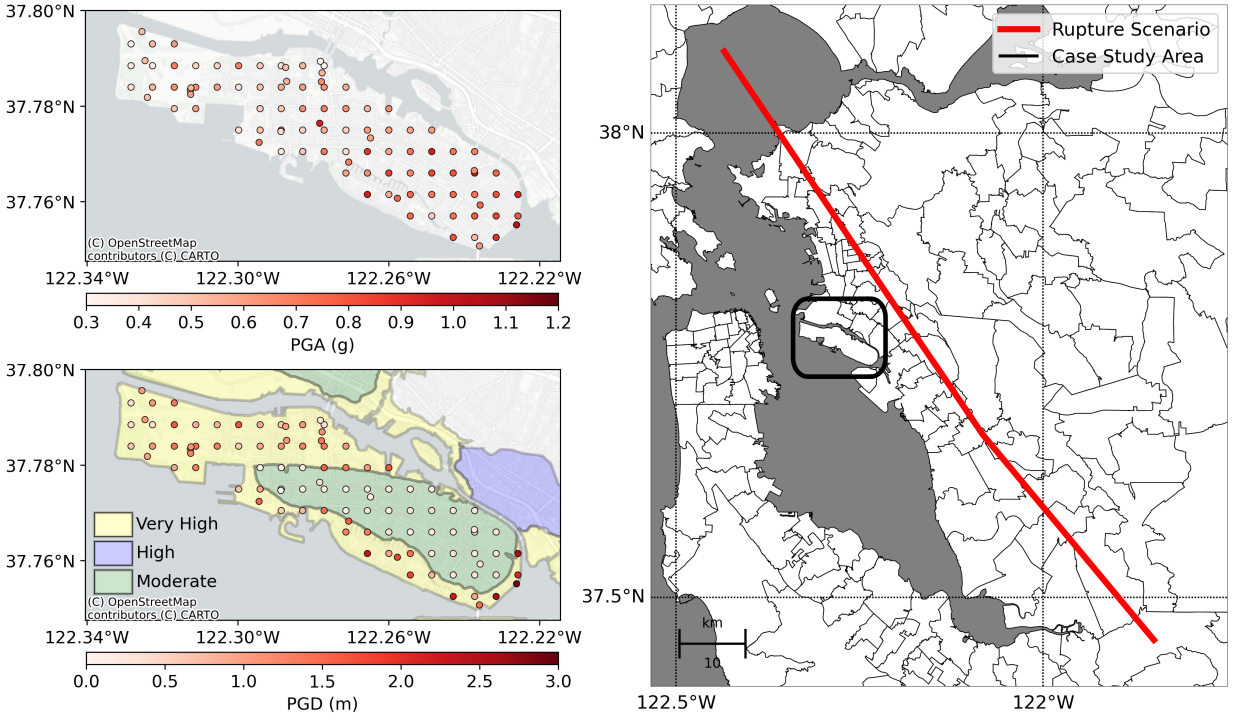

Figure 4: Case study hazard scenario. Upper left: Estimated peak ground acceleration (PGA) at a suite of grid points in the case study area. Lower left: Estimated soil liquefaction permanent ground deformation (PGD) in the case study area. The color stands for the liquefaction susceptibility of the corresponding geologic unit [46]. Right: The locations of the M_w 7.0 fault rupture scenario and the studied area.

acceleration at 0.3 s and 1.0 s, are estimated using the ground motion prediction equation developed by [1], the inter-event correlation model proposed by [5], and the intra-event correlation model from [17]. These ground motion models are stochastic, and one realization of the ground shaking IM, which complies with the above ground motion models, is selected for this case study (see Fig. 4). Using this ground-shaking IM realization, the soil liquefaction-induced permanent ground deformation (PGD) is estimated using the geology-based method suggested in FEMA HAZUS [20], with soil liquefaction susceptibility determined from the geologic map developed by [46].

The building inventory is developed by [6], using data collected from open-source databases [35, 42] and augmented with machine learning models based on street view images. The inventory augmentation models are accessed through SimCenter's BRAILS++ tool [14]. A highway transportation inventory is also created using BRAILS++, with public data retrieved from the National Bridge Inventory, National Tunnel Inventory, and TigerWeb [18, 41]. The asset information for the water distribution network (WDN) is not publicly available, so a hypothetical WDN inventory was created. Pipeline locations were assumed to align with roads in the transportation inventory, an arbitrary water source was assumed, and demand was estimated using local census data. The infrastructure inventory used in this case study is shown in Fig. 5 and is openly available (see the Data Availability section).

To estimate the damage states of the infrastructure components in Fig. 5, simple damage functions in the form of fragility curves, as defined by HAZUS [20], are used. The Python package Pelicun [51], integrated into the R2D software, is employed to generate damage state realizations according to the FEMA HAZUS damage functions.

Fig. 6 shows one of the damage state realizations sampled based on the ground shaking and ground failure intensity, as presented in Fig. 4. The description of the damage states is available in [20]. The damage is significant due to the proximity of the studied area to the hypothetical earthquake scenario, which represents nearly the largest possible earthquake on the Hayward fault. Additionally, the reclaimed land in the studied region has very high soil liquefaction susceptibility [6], resulting in considerable damage from ground failure and permanent ground deformation.

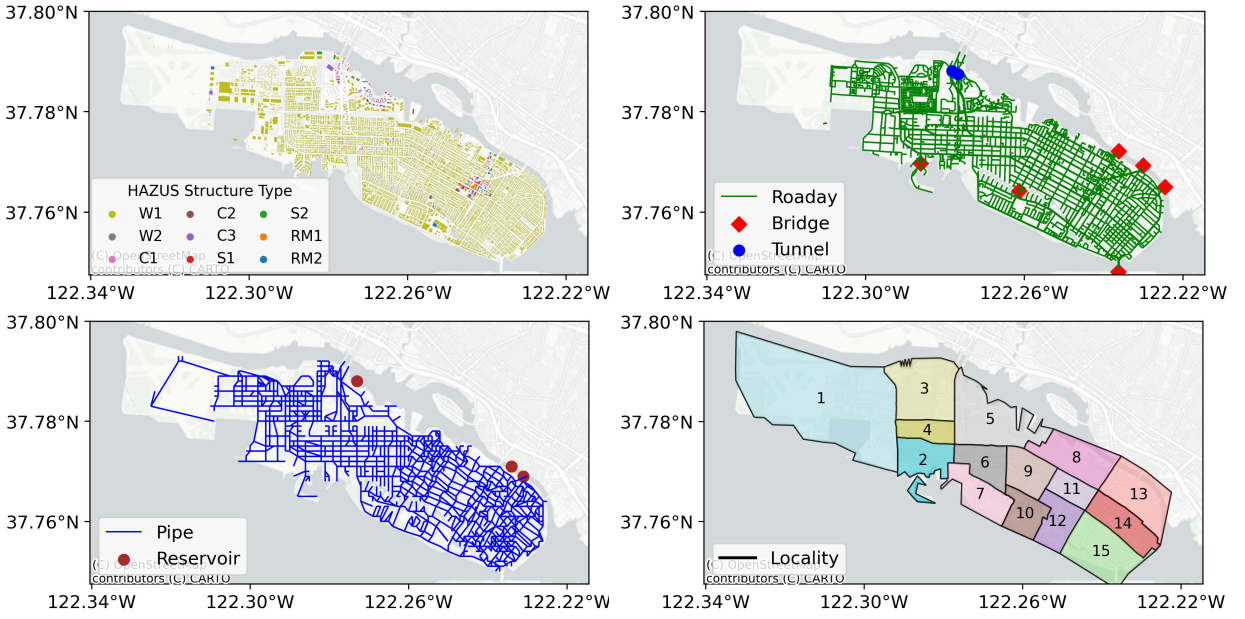

Figure 5: Case study infrastructure inventory. Upper left: Building stocks. Upper right: Transportation infrastructure. Lower left: Potable water distribution infrastructure. Lower right: Simulation locality, modified from the MTC travel analysis zones [33]. The building structure types are defined in the HAZUS Inventory Technical Manual [19]

3.2. Recovery simulation utilizing infrastructure system operation simulators

The primary objective of this case study is to evaluate the system-level performance of infrastructure systems during recovery and to model the interdependencies among buildings, the water system, and the transportation system, using infrastructure simulators that comply with physical and technical resource distribution laws. Operational resources considered include potable water and transportation services, while recovery resources consist of engineers, funding, contractors, and repair crews. Building recovery sequences are informed by observations from the 1994 Northridge earthquake [39]. Recovery resource supply capacities are assumed by the authors and provided in the supplement data (see Data Availability section). Residential water demand is linked to the number of occupants in a building and varies with the building's shelter capacity as recovery progresses. Shelter capacity depends on both the initial damage state and recovery status: buildings with no or minor damage retain full shelter capacity throughout recovery, whereas those with moderate, severe, or complete damage provide no shelter until repairs are completed.

Fig. 7 and Fig. 8 illustrate the status of all infrastructure 30 days and 150 days after the studied earthquake event, with the infrastructure status at various time steps provided in the supplement data.

The distribution of potable water is simulated using REWET and the developed API. At each recovery simulation timestep, pyrecodes sends each component's functionality and new population data to the API, which estimates the new demand at each node and creates the input data for REWET. REWET then runs EPANET V2.2 to simulate the water flow every 5 days for the initial 50 days after the earthquake, every 10 days for the following 150 days, and every 50 days thereafter. The API calculates the satisfied demand for each building. The leak models, based on the material (assumed to be brittle iron in this case study) and other hydraulic solver parameters, are taken to be the default values defined in REWET [34]. Fig. 9 presents the potable water supply and demand recovery curve for the studied area.

The Residual Demand simulator and the accompanying API are used to dynamically evaluate the performance of the transportation network throughout the recovery process. The system simulation is conducted every 5 days during the first 50 days after the hazard event, every 20 days in the following 150 days, and every 50 days thereafter until all components have recovered to their pre-disaster level. At each simulation step, the Residual Demand API estimates the population reduction in each locality based on housing recovery progress and adjusts the pre-disaster travel demand proportionally to the population reduction. The population from each building is assigned to a locality, and the total population in the locality (referred to as the locality population) is calculated. The ratio of post-disaster to pre-disaster locality populations is then computed for each locality, and the number of trips originating from, or destined to,

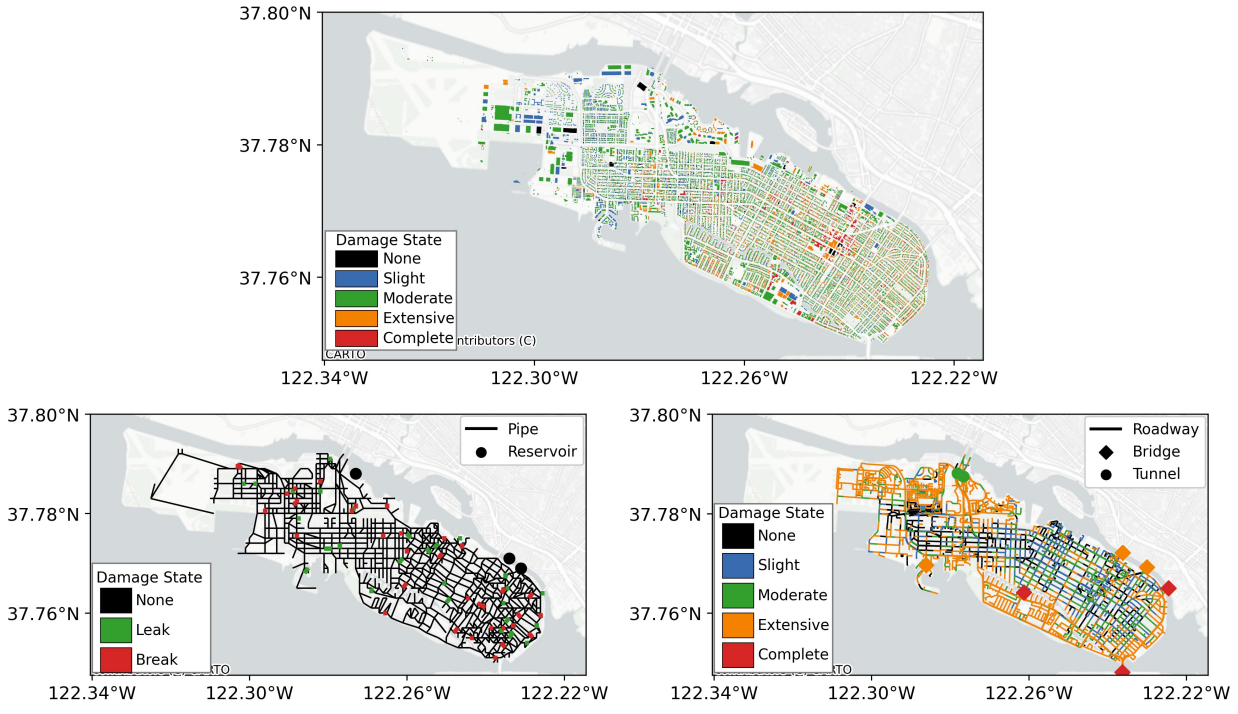

Figure 6: Damage state immediately after the case study earthquake. Top: Building stock. Bottom left: Potable water distribution infrastructure. Bottom right: Transportation infrastructure.

that locality is reduced by the same ratio as the population reduction. Note that these travel demand assumptions are oversimplified, and there is a need for more realistic post-disaster travel demand models from the transportation and social science research community. Once available, such travel demand models could be readily incorporated into this simulation framework. However, for now, these simple models are useful to generate qualitative results that demonstrate the utility of the proposed framework.

To estimate the network capacity at each recovery time step, the capacity and maximum speed of roadways are adjusted according to the recovery progress and functionality level of the roads and the bridges or tunnels that support them. Roads and bridges that experienced damage are conservatively assumed to be fully closed until repaired. The travel time for each trip in the updated travel demand is then estimated using the dynamic traffic assignment simulation in Residual Demand. In this case study, a trip is considered incomplete if the post-disaster travel time is more than three times longer than the pre-disaster travel time. The number of demanded and completed trips during the recovery process is plotted in Fig. 9 (right).

3.3. Discussion

The case study demonstrates that the integrated simulation platform enables modeling of both the potential damage from an earthquake event and the recovery process of a community, considering multiple interdependent infrastructure systems. Due to the close proximity to the hypothetical earthquake event, the ground shaking intensity is high, with an average peak ground acceleration (PGA) of 0.62 g. This intense ground shaking caused significant damage to the building stock, with nearly all buildings experiencing some damage, and 26% of the buildings experiencing extensive or complete damage. The high ground shaking also led to considerable soil liquefaction in the near-shore areas, which have very high liquefaction susceptibility (see Fig. 4). Roadways and bridges are particularly vulnerable to ground deformation [20], resulting in extensive liquefaction-induced damage. In contrast, the water pipelines, which are buried underground, were less vulnerable to ground shaking and ground deformation. Consequently, only a moderate number of pipeline breaks and leaks were predicted.

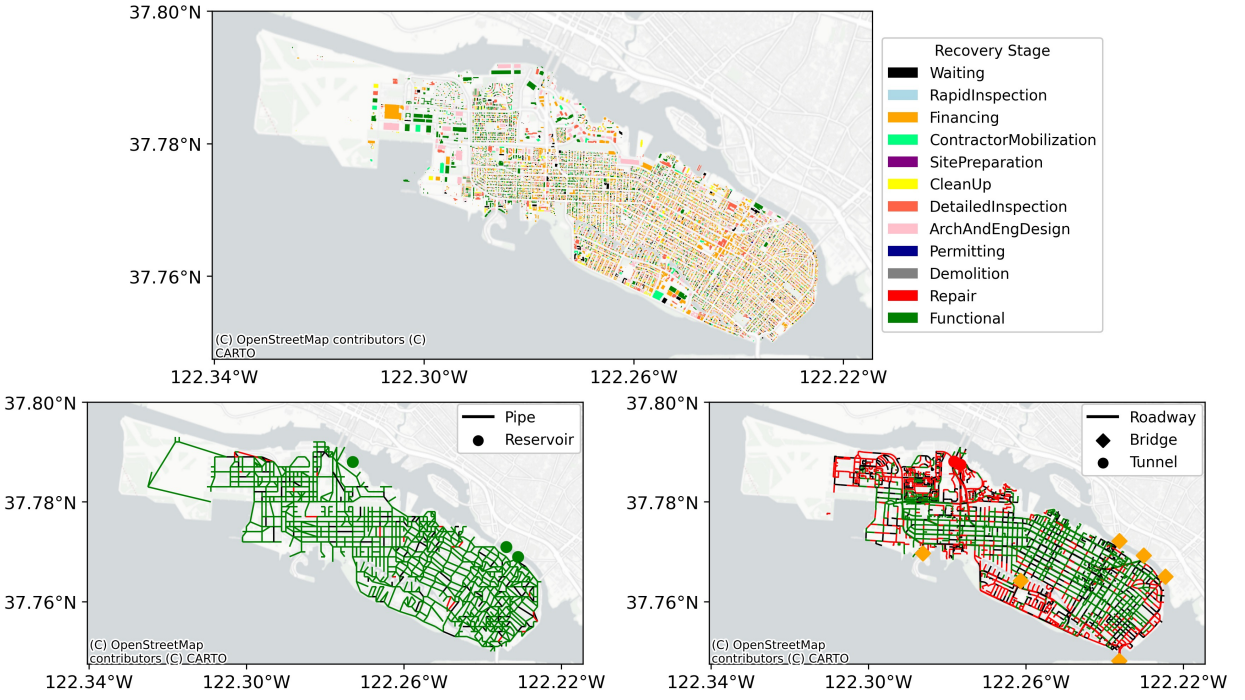

Figure 7: Damage and recovery state of infrastructure components 30 days after the earthquake.

Fig. 7 shows that 30 days after the earthquake, most houses and bridges are undergoing pre-repair activities, such as financing and design, while damaged roads and pipelines have already started the repair process. By 150 days post-earthquake (see Fig. 8), all pipelines and roadways have fully recovered and been restored to functional status. A large number of slightly and moderately damaged buildings have also been restored to functionality. However, the severely damaged buildings (e.g., in locality 11, as shown in Fig. 5) and bridges are still under repair. This delay is due to the lengthy financing, design, demolition, and repair processes required for the recovery of heavily damaged buildings and bridges. In this case study, it took a total of 485 days for all infrastructure components to complete the recovery process under the assumed recovery conditions. Please note that the assumed recovery conditions are optimistic, as a high supply of recovery resources is assumed, resulting in a relatively short recovery time. A more realistic recovery assessment would require refinement of the recovery resource supply assumptions.

Fig. 9 illustrates the resilience of the roadway transportation network during the hypothetical earthquake event. Following the earthquake, travel demand decreased due to building damage and the relocation of people. The number of completed trips also dropped due to extensive damage to roadways and bridges. The pre-disaster travel demand was derived from a simulation model developed by the San Francisco Bay Area Metropolitan Transportation Commission (MTC), which models typical weekday travel to assist in regional planning activities [32]. A significant portion of the travel demand originates from or is destined toward the mainland, requiring access to one of the region's bridges or tunnels. As the bridges were heavily damaged and took approximately 450 days to fully repair, a large number of trips had to be rerouted, resulting in a significant unmet travel demand. This underscores the critical role that bridges play in the resilience of the transportation network. Furthermore, the recovery of transportation service supply was slower than the recovery of housing and travel demand in the region, highlighting the importance of prioritizing recovery efforts in natural hazard events. These insights may inform the decision-making for recovery scheduling and resource allocation in the aftermath of disasters.

Fig. 9 illustrates the variation in potable water demand and supply during the recovery process. Both water demand and supply dropped significantly after the earthquake. The change in water demand is due to the damage and reduced occupancy of the buildings. As buildings are repaired and residents return, water demand increases. The water supply initially falls short of demand. However, in this case study, around 150 days after the earthquake, all damaged pipes are repaired, and water delivery services are fully restored, eliminating unmet water demand in the region.

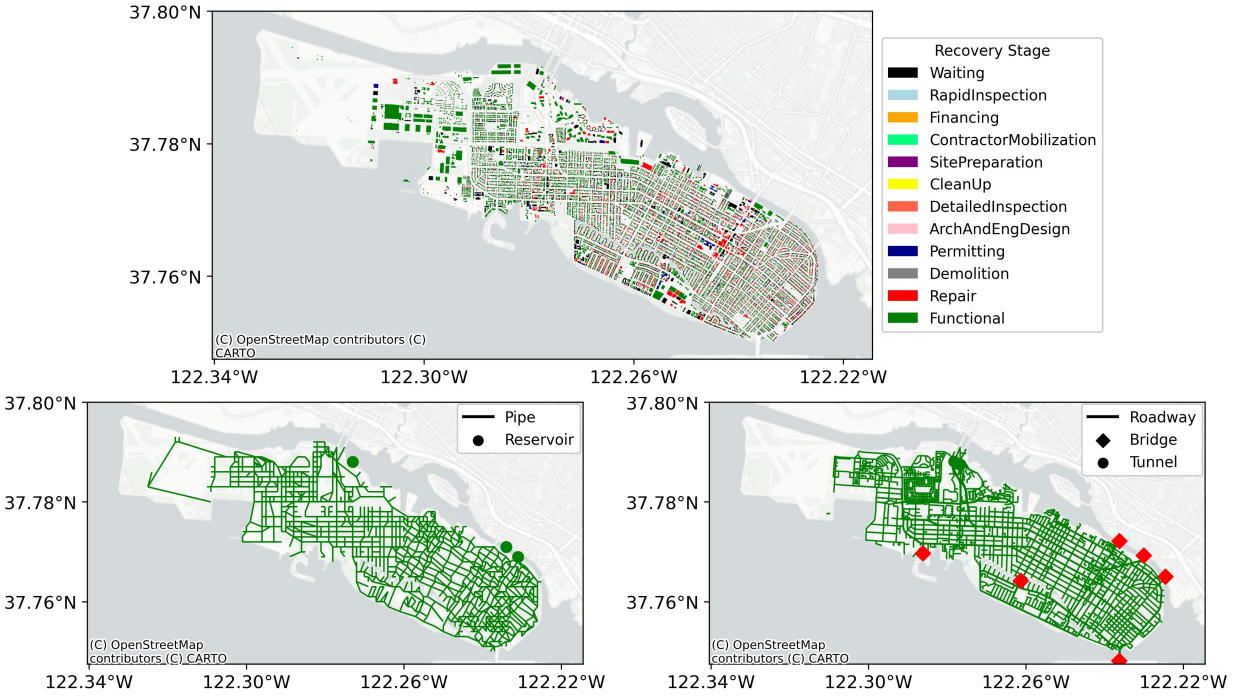

Figure 8: Damage and recovery state of infrastructure components 150 days after the earthquake.

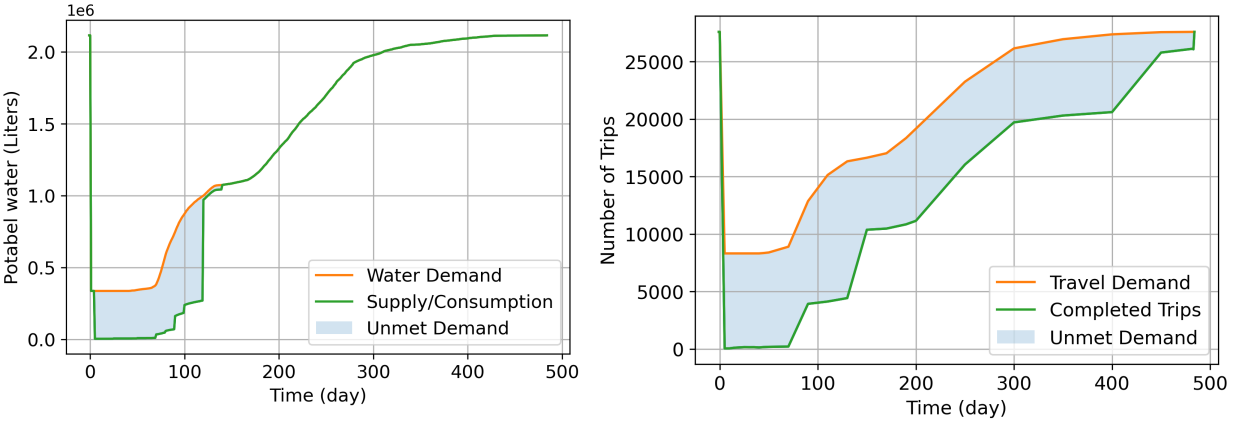

Figure 9: Supply/Consumption and demand recovery curves for the studied area. Left: Potable Water; Right: Transportation Service

Fig. 10 compares the variation in potable water supply and demand in locality 3 and locality 11 (see Fig. 5, bottom right). Due to pipeline damage, the water supply in both localities was significantly reduced after the earthquake. However, water demand in locality 3 decreased by a smaller percentage than in locality 11 due to the smaller extent of building damage in locality 3 (see Fig. 6). As a result, locality 3 experienced a larger unmet water demand and, consequently, a greater lack of resilience in water delivery services compared to locality 11. This information suggests that additional water resources should be directed to locality 3, and the restoration of water delivery services in this area should be prioritized. This comparison highlights the importance of considering the interaction between supply and demand across multiple infrastructure systems when evaluating community resilience and making emergency response plans. Simulating such interactions would be challenging without the integrated platform developed in this paper.

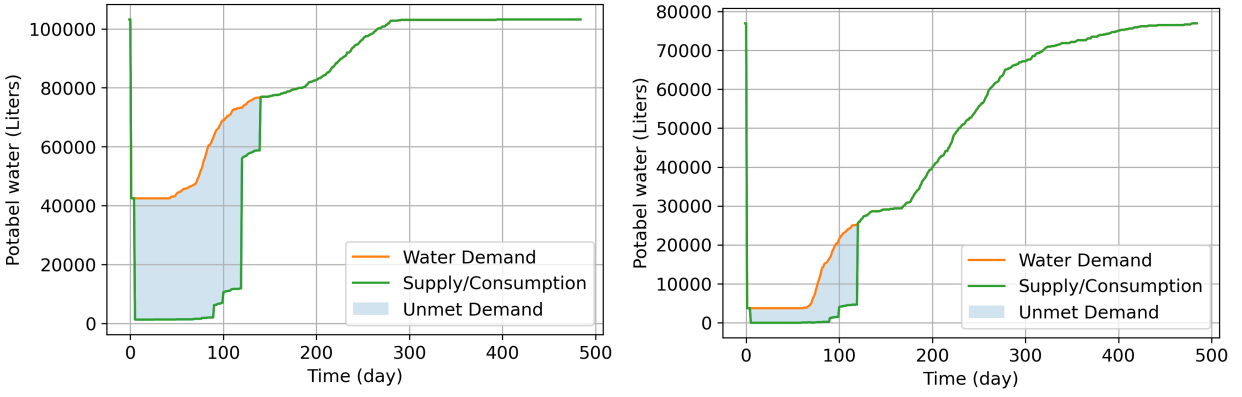

Figure 10: Potable water supply/consumption and demand recovery curves. Left: Locality 3; Right: Locality 11.

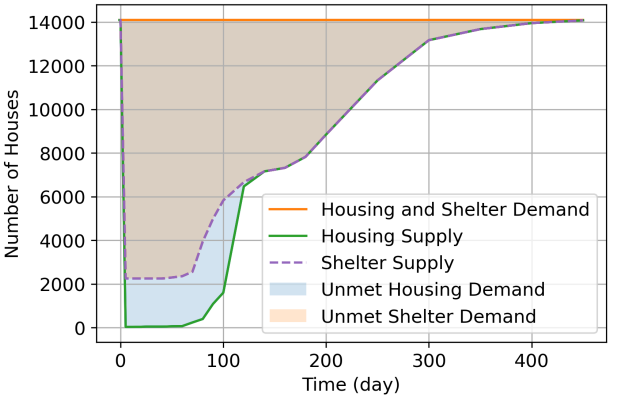

Figure 11: Functional housing and shelter supply/consumption and demand recovery curves.

The water demand model used in this case study may still be considered as simplified because it does not account for water consumption due to repair activities. Additionally, although the buildings are non-functional, temporary shelters are likely to be established after major earthquake events, but water demands from these shelters are not included in the model. Nevertheless, the case study demonstrates that the simulation platform effectively captures the dynamics of water demand and supply, and the assumptions made in the water demand model are reflected in the simulation results. More detailed water demand assumptions and models could be developed through collaboration with utilities and municipalities creating resilience plans, and these could be implemented in the pyrecodes-REWET API introduced in this paper.

Fig. 11 illustrates the recovery of shelters and functional houses on the island. In this case study, a building is considered a shelter once all prescribed recovery activities are completed, and it becomes functional housing when its operational demands (primarily potable water) are met. Immediately after the earthquake, about 20% of buildings are occupiable and are used as shelters. However, due to the sharp reduction in water supply (see Fig. 9), almost none of the buildings are fully functional. Shelter demand remains roughly constant during the first 50 days while pre-repair and repair activities are underway (e.g., Fig. 7). Shelter supply begins to increase around day 60 and gradually recovers to meet total demand. In contrast, functional housing lags behind during the first 100 days, constrained by ongoing water system repairs. By around day 150, when water delivery services are fully restored, all shelters transition into functional housing, causing the two recovery curves to converge. This analysis highlights another value of the integrated platform in simulating interdependent infrastructure systems: differentiating between shelter and housing supply can inform population relocation and economic recovery analyses, which further underscores the importance of modeling cross-infrastructure interactions.

4. Conclusions

This paper presents an open-source integrated simulation platform designed to model the resilience of interdependent infrastructure systems following natural hazards. The platform integrates SimCenter's regional resilience determination (R2D) tool and ETH Zurich's recovery simulation tool, pyrecodes, through innovative application programming interfaces (APIs). The system-to-system APIs developed in this paper interface the pyrecodes recovery simulation with system performance models, which enables a dynamic and comprehensive evaluation of infrastructure recovery under the constraints of operational and recovery resources. The simulation platform and APIs are open-source and flexible, allowing for the extension to incorporate newer and more advanced models, thereby further improving the accuracy and reliability of the simulation results. Moreover, they provide a framework for unifying diverse research efforts, from hazard simulation to recovery modeling, ultimately advancing our understanding and assessment of infrastructure resilience and supporting better disaster preparedness, recovery planning, and sustainable development.

A case study based on a hypothetical earthquake scenario demonstrates the platform's ability to simulate potential infrastructure damage, the recovery process, and the dynamic interdependencies among infrastructure systems. Furthermore, the case study highlights the critical importance of considering interdependencies among infrastructure systems, such as buildings, water distribution, and transportation networks, when assessing community resilience. The simulation platform that integrates hazard, exposure, vulnerability, recovery and infrastructure operations simulators through the presented APIs shows great potential to improve community resilience assessment and enhancement through its ability to include interdependencies in the modeling and simulation of recovery strategies. The developed platform and the case study, with all associated data, models, and source code, are thoroughly documented and made publicly available. The case study is intended to serve not only as a demonstration of the proposed framework, but also as a reproducible and extensible testbed for the broader resilience research community. By providing a well-documented simulation tool and an end-to-end example, the study lowers the barrier for other researchers to adopt, validate, benchmark, and extend the proposed methodology in future resilience analyses.

Data availability

- A compiled simulation software can be downloaded from https://simcenter.designsafe-ci.org/research-tools/r2dtool/.
- The source code of R2D simulation: https://github.com/NHERI-SimCenter/SimCenterBackendApplications.
- The source code of pyrecodes: https://github.com/NikolaBlagojevic/pyrecodes
- The source code of R2D user interface: https://github.com/NHERI-SimCenter/R2DTool.git
- The input and output of the case study simulation can be found at: Integrated Regional Resilience Assessment Platform for Interdependent Systems. DesignSafe-CI. https://doi.org/10.17603/ds2-yhht-3076 .

Relevance to resilience

The simulation platform presented in this paper is highly relevant to resilience assessment because it links probabilistic hazard and damage estimation with dynamic, system-level recovery processes. The damage module provides high-resolution, uncertainty-aware estimates of infrastructure damage and functionality loss across spatially distributed assets under natural hazards. The recovery module simulates the subsequent post-event recovery by explicitly modeling interdependencies among infrastructure systems, resource constraints, and repair sequencing over time. The integrated framework enables quantifying resilience not only in terms of immediate performance loss but also through repair, service restoration, and community-level functional recovery. This integration is essential for assessing the resilience of urban systems from pre-event risk, through post-event disruption, to long-term recovery, within a consistent probabilistic and computational framework, thereby supporting more informed decision-making for mitigation, planning, and investment prioritization. The presented simulation platform is fully open-source, allowing further expansion to include more comprehensive infrastructure system simulators.

Acknowledgments

The authors acknowledge the funding from the NHERI-SimCenter (NSF award numbers 1612843 and 2131111) and from ETH Zurich that enabled work on R2D and pyrecodes, respectively. The authors would like to express their gratitude to everyone at the NHERI-SimCenter, Singapore ETH Center, and ETH Zurich for their valuable comments and for their contributions to the development of SimCenter and ETH Zurich tools.

References

[1] Abrahamson, N.A., Silva, W.J., Kamai, R., 2014. Summary of the ASK14 ground motion relation for active crustal regions. Earthquake Spectra 30, 1025–1055.

[2] Ahmed, S., Dey, K., 2020. Resilience modeling concepts in transportation systems: a comprehensive review based on mode, and modeling techniques. Journal of Infrastructure Preservation and Resilience 1, 8.

[3] Alisjahbana, I., Kiremidjian, A., 2021. Modeling housing recovery after the 2018 lombok earthquakes using a stochastic queuing model. Earthquake Spectra 37, 587–611.

[4] Angeles, K., Kijewski-Correa, T., 2023. Advancing parcel-level hurricane regional loss assessments using open data and the regional resilience determination tool. International Journal of Disaster Risk Reduction 95, 103818.

[5] Baker, J.W., Bradley, B.A., 2017. Intensity measure correlations observed in the NGA-West2 database, and dependence of correlations on rupture and site parameters. Earthquake Spectra 33, 145–156.

[6] Bassman, T., Zsarnóczay, A., Saw, J., Wang, S., Deierlein, G., 2022. High-fidelity testbed development for regional risk assessment in alameda, california, in: 12th National Conference on Earthquake Engineering.

[7] Blagojević, N., Didier, M., Stojadinović, B., 2022a. Evaluating NIST community disaster resilience goals using the ire-codes resilience quantification framework, in: Proceedings of 12 national conference on earthquake engineering, Earthquake Engineering Research Institute (EERI) Salt Lake City, Utah.

[8] Blagojević, N., Didier, M., Stojadinović, B., 2022b. Risk-informed resilience assessment of communities using lack of resilience surfaces, in: Proceedings of 13th international conference on structural safety and reliability (ICOSSAR 2021).

[9] Blagojević, N., Hefti, F., Henken, J., Didier, M., Stojadinović, B., 2023. Quantifying disaster resilience of a community with interdependent civil infrastructure systems. Structure and Infrastructure Engineering 19, 1696–1710.

[10] Blagojević, N., Lauber, N., Didier, M., Stojadinović, B., 2022c. Evaluating the importance of interdependent civil infrastructure system components for disaster resilience of community housing, in: Lifelines 2022. ASCE, pp. 927–937.

[11] Blagojević, N., Stojadinović, B., 2022. A demand-supply framework for evaluating the effect of resource and service constraints on community disaster resilience. Resilient Cities and Structures 1, 13–32.

[12] Blagojević, N., Stojadinovic, B., 2025. pyrecodes: an open-source library for regional recovery simulation and disaster resilience assessment of the built environment (v0.2.0).

[13] Ceferino, L., Kukunoor, C., Zhao, J., Mao, D., Xu, X., Wu, J., Zsarnóczay, A., 2025. Accessing acute care hospitals in the san francisco bay area after a major hayward earthquake. Nature Communications 16, 9328.

[14] Cetiner, B., McKenna, F., Yi, S.r., Wang, B., Manousakis, I.V., 2025. Brails++. URL: https://doi.org/10.5281/zenodo.17203241, doi:10.5281/zenodo.17203241.

[15] Cimellaro, G., Arcidiacono, V., Reinhorn, A., 2021. Disaster resilience assessment of building and transportation system. Journal of Earthquake Engineering 25, 703–729.

[16] Costa, R., Haukaas, T., 2021. The effect of resource constraints on housing recovery simulations. International journal of disaster risk reduction 55, 102071.

[17] Du, W., Ning, C.L., 2021. Modeling spatial cross-correlation of multiple ground motion intensity measures (SAs, PGA, PGV, Ia, CAV, and significant durations) based on principal component and geostatistical analyses. Earthquake Spectra 37, 486–504.

[18] Federal Highway Administration, 2025. National bridge inventory (NBI). URL: https://www.fhwa.dot.gov/bridge/nbi.cfm. accessed: 2025-07-20.

[19] FEMA, 2020. Hazus Inventory Technical Manual. URL: https://www.fema.gov/hazus. accessed: 2025-06-03.

[20] FEMA, 2024. HAZUS Earthquake Technical Manual. Technical Report. Federal Emergency Management Agency (FEMA). Washington, D.C.

[21] Field, E.H., Dawson, T.E., Felzer, K.R., Frankel, A.D., Gupta, V., Jordan, T.H., Parsons, T., Petersen, M.D., Stein, R.S., Weldon, R., et al., 2009. Uniform california earthquake rupture forecast, version 2 (UCERF 2). Bulletin of the Seismological Society of America 99, 2053–2107.

[22] Field, E.H., Jordan, T.H., Cornell, C.A., 2003. OpenSHA: A developing community-modeling environment for seismic hazard analysis. Seismological Research Letters 74, 406–419.

[23] Klise, K., Hart, D., Bynum, M., Hogge, J., Haxton, T., Murray, R., Burkhardt, J., 2020. Water network tool for resilience (WNTR). User manual, version 0.2. 3. Technical Report. Sandia National Lab.(SNL-NM), Albuquerque, NM (United States).

[24] van de Lindt, J.W., Kruse, J., Cox, D.T., Gardoni, P., Lee, J.S., Padgett, J., McAllister, T.P., Barbosa, A., Cutler, H., Van Zandt, S., et al., 2023. The interdependent networked community resilience modeling environment (IN-CORE). Resilient Cities and Structures 2, 57–66.

[25] Lu, X., McKenna, F., Cheng, Q., Xu, Z., Zeng, X., Mahin, S.A., 2020. An open-source framework for regional earthquake loss estimation using the city-scale nonlinear time history analysis. Earthquake Spectra 36, 806–831.

[26] Luettich, R.A., Westerink, J.J., Scheffner, N.W., et al., 1992. ADCIRC: An advanced three-dimensional circulation model for shelves, coasts, and estuaries. report 1. theory and methodology of ADCIRC-2DDI and ADCIRC-3DL. .

[27] Masoomi, H., Burton, H., Tomar, A., Mosleh, A., 2020. Simulation-based assessment of postearthquake functionality of buildings with disruptions to cross-dependent utility networks. Journal of Structural Engineering 146, 04020070.

[28] McCallen, D., Petersson, A., Rodgers, A., Pitarka, A., Miah, M., Petrone, F., Sjogreen, B., Abrahamson, N., Tang, H., 2021. EQSIM—a multidisciplinary framework for fault-to-structure earthquake simulations on exascale computers part i: Computational models and workflow. Earthquake Spectra 37, 707–735.
[29] McKenna, F., Gavrilovic, S., Zhao, J., Zhong, K., Zsarnoczay, A., Cetiner, B., Naeimi, S., Yi, S.r., Bangalore Satish, A., Arduino, P., 2024. NHERI-SimCenter/R2DTool: Version 5.1.0.
[30] McKenna, F., Gavrilovic, S., Zhao, J., Zhong, K., Zsarnoczay, A., Cetiner, B., Naeimi, S., Yi, S.r., Bangalore Satish, A., Arduino, P., 2025a. Asset Analysis. URL: https://nheri-simcenter.github.io/R2D-Documentation/common/user_manual/usage/desktop/R2DTool/ANA.html#ana-asset-analysis. accessed: 2025-08-25.
[31] McKenna, F., Gavrilovic, S., Zhao, J., Zhong, K., Zsarnoczay, A., Cetiner, B., Naeimi, S., Yi, S.r., Bangalore Satish, A., Arduino, P., 2025b. Earthquake Event Simulation. URL: https://nheri-simcenter.github.io/R2D-Documentation/common/user_manual/usage/desktop/R2DTool/tools.html#earthquake-event-simulation. accessed: 2025-08-25.
[32] Metropolitan Transportation Commission, 2022. Mtc/abag forecasting, modeling surveys: Data repository. URL: https://data.mtc.ca.gov/data-repository/. accessed: 2025-05-04.
[33] Metropolitan Transportation Commission, 2023. Transportation analysis zone. https://opendata.mtc.ca.gov/datasets/MTC::transportation-analysis-zones/about. Accessed: 2025-04-02.
[34] Naeimi, S., 2023. Post-event restoration simulation of water distribution systems: A generally applicable approach. University of Delaware.
[35] OpenStreetMap contributors, 2017. Planet dump retried from https://planet.osm.org. https://planet.osm.org. Accessed: 2025-04-02.
[36] Pagani, M., Monelli, D., Weatherill, G., Danciu, L., Crowley, H., Silva, V., Henshaw, P., Butler, L., Nastasi, M., Panzeri, L., et al., 2014. OpenQuake engine: An open hazard (and risk) software for the global earthquake model. Seismological Research Letters 85, 692–702.
[37] Sharma, N., Tabandeh, A., Gardoni, P., 2020. Regional resilience analysis: A multiscale approach to optimize the resilience of interdependent infrastructure. Computer-Aided Civil and Infrastructure Engineering 35, 1315–1330.
[38] Snaiki, R., Wu, T., 2017. A linear height-resolving wind field model for tropical cyclone boundary layer. Journal of Wind Engineering and Industrial Aerodynamics 171, 248–260.
[39] Terzic, V., Villanueva, P.K., Saldana, D., Yoo, D.Y., 2021. Framework for modelling post-earthquake functional recovery of buildings. Engineering Structures 246, 113074. URL: https://www.sciencedirect.com/science/article/pii/S0141029621012116, doi:https://doi.org/10.1016/j.engstruct.2021.113074.
[40] Tomar, A., Burton, H.V., Mosleh, A., Yun Lee, J., 2020. Hindcasting the functional loss and restoration of the napa water system following the 2014 earthquake using discrete-event simulation. Journal of Infrastructure Systems 26, 04020035.
[41] U.S. Census Bureau, 2025a. TIGERweb. URL: https://tigerweb.geo.census.gov/tigerwebmain/TIGERweb_main.html. accessed: 2025-07-20.
[42] U.S. Census Bureau, 2025b. United states census bureau. https://www.census.gov/. Accessed: 2025-04-02.
[43] U.S. Environmental Protection Agency, 2025. Epanet. URL: https://www.epa.gov/water-research/epanet. accessed: 2025-07-20.
[44] Wald, D.J., Worden, C.B., Thompson, E.M., Hearne, M., 2022. ShakeMap operations, policies, and procedures. Earthquake Spectra 38, 756–777.
[45] Wang, W.L., van de Lindt, J.W., 2021. Quantitative modeling of residential building disaster recovery and effects of pre-and post-event policies. International Journal of Disaster Risk Reduction 59, 102259.
[46] Witter, R.C., Knudsen, K.L., Sowers, J.M., Wentworth, C.M., Koehler, R.D., Randolph, C.E., Brooks, S.K., Gans, K.D., 2006. Maps of Quaternary deposits and liquefaction susceptibility in the central San Francisco Bay region, California. Technical Report. US Geological Survey.
[47] Xiong, C., Huang, J., Lu, X., 2020. Framework for city-scale building seismic resilience simulation and repair scheduling with labor constraints driven by time–history analysis. Computer-Aided Civil and Infrastructure Engineering 35, 322–341.
[48] Zhang, W., Restrepo, D., Crempien, J.G., Erkmen, B., Taborda, R., Kurtulus, A., Taciroglu, E., 2021. A computational workflow for rupture-to-structural-response simulation and its application to istanbul. Earthquake Engineering & Structural Dynamics 50, 177–196.
[49] Zhao, B., Kumar, K., Casey, G., Soga, K., 2019. Agent-based model (ABM) for city-scale traffic simulation: A case study on San Francisco, in: International Conference on Smart Infrastructure and Construction 2019 (ICSIC) Driving data-informed decision-making, ICE Publishing. pp. 203–212.
[50] Zhou, Y., Wang, J., Yang, H., 2019. Resilience of transportation systems: concepts and comprehensive review. IEEE Transactions on Intelligent Transportation Systems 20, 4262–4276.
[51] Zsarnoczay, A., Manousakis, J.V., Zhao, J., Naeimi, S., Kourehpaz, P., Zhong, K., McKenna, F., Cetiner, B., kanwardhindsa, 2025. NHERI-SimCenter/pelicun: v3.6.1. URL: https://doi.org/10.5281/zenodo.15447502, doi:10.5281/zenodo.15447502.